

RESEARCH

Open Access



# 3D flame reconstruction and error calculation from a schlieren projection

C. Alvarez-Herrera<sup>1\*</sup> , J. L. Herrera-Aguilar<sup>1</sup>, D. Moreno-Hernández<sup>2</sup>, A. V. Contreras-García<sup>1</sup> and J. G. Murillo-Ramírez<sup>3</sup>

## Abstract

In this work a 3D flame reconstruction is performed from a 2D projection of the hot gases of a combustion flame. The projection is obtained using an optical schlieren technique. In this technique, a schlieren image is integrated linearly to obtain the hot gases, and then, a temperature field. Each row of the matrix representing the temperature distribution is fitted with a specific function, and its respective error is calculated. In this way, the projected matrix can be represented with the fitted functions. As a result of the procedure used in this research, a slice of the flame is obtained by assuming a cylindrical symmetry of it and multiplying the fitted function by itself. Finally, it was evaluated the mean error in calculations of temperature intensity in the flame under the cylindrical symmetry assumption obtaining an accuracy of 96% which validates the efficiency of our method.

**Keywords:** 3D flame reconstruction, Schlieren technique

## Introduction

Nowadays, combustion flames are an important subject of study due to its importance in technology, fluctuations in oil prices and air pollution due to combustion processes. Therefore, these reasons are good motivations to look for efficiency in flames. Furthermore, fossil fuels are a finite reservoir of energy that each day decreases continuously in the world [1]. Because of these reasons, it is important to increase the efficiency in combustion flames to reduce fuel consumption in such a way that it will be decrease greenhouse effect and saving money by less fuel consumption. Hence, to have a better understanding of combustion of flames several optical nondestructive full field techniques are used such as; interferometry arrangements in form of tomography, shadowgraph and schlieren [2].

The schlieren techniques quantify the ray deviation at the observation plane. The ray deviates due to changes in the refractive index caused by temperature variations. This technique is used in this manuscript to analyze the

hot gases produced by the combustion in flames, and to obtain the shape of flame. Schlieren technique is commonly used in wind tunnels for aeronautic and flame diagnostic since it is suitable and easy to implement [2, 3]. Real combustion flames are compounds of hot gases distributed in a volume, and flame temperature is one of the parameters which can be used to determine the efficiency of combustion processes. However, the schlieren technique obtains information which is integrated along an optical path. Thus, the schlieren technique quantifies the refractive index gradients in a projection plane caused by the hot gases distributed inside a volume. The resultant image at the observation plane contains three dimensional information of the hot gases. Although the information at the projected plane is commonly useful, it is important to calculate the three dimensional information of the volumetric object. In order to determine this information, some authors used projections at different angles to reconstruct a volumetric object using the Radon transform [4]. Other authors used the assumption of cylindrical geometry to apply the Abel transform [5], as it was done in this work to obtain a volumetric reconstruction of an object.

\*Correspondence: [calvarez@uach.mx](mailto:calvarez@uach.mx)

<sup>1</sup>Facultad de Ingeniería, Universidad Autónoma de Chihuahua, Nuevo Campus Universitario, Circuito Universitario S/N, 31125, Chihuahua, Chih., México  
Full list of author information is available at the end of the article

It is well known that flames do not have perfect cylindrical shape and to calculate the error is very important to have a real measurement of the accuracy of the reconstruction. In this work, the three-dimensional flame reconstruction includes an error which was evaluated. The main goal of this work was to perform a three-dimensional reconstruction of a flame starting from a 2D projection of hot gases using an easy and novel mathematical method based on schlieren techniques and under the assumption of cylindrical symmetry of the temperature spatial distribution in the flame.

### Theoretical background

The three-dimensional reconstruction of a flame in the present work uses the schlieren optical technique to data acquisition in form of refractive index gradient and it also uses the assumption of cylindrical geometry to process the results.

#### Schlieren technique theory

Schlieren technique was used to acquire the visualization of gradient of refractive index in two-dimensions caused by the hot gases in a combustion flame. The light ray propagation through a transparent media was used to describe how schlieren technique works, as shown in Fig. 1. When a light ray travels through a transparent media with a thickness  $W = \zeta_2 - \zeta_1$  and a refractive index  $n = n(x, y, z)$  it experiences certain deflection angle forming a projection of the object in the image plane. The ray propagation in an inhomogeneous medium is well described by the eikonal equation given by [1, 2, 6]:

$$\frac{d}{ds} \left( n \frac{d\mathbf{r}}{ds} \right) = \nabla n. \quad (1)$$

Where  $ds$  is the arc length defined as  $ds^2 = dx^2 + dy^2 + dz^2$  and  $\mathbf{r}$  is a position vector. The light ray passes through the inhomogeneous medium in the  $z$ -direction from  $\zeta_1$  to  $\zeta_2$  changing  $ds$  into  $dz$  each displacement of  $dz$  generates a small angle deflection. Assuming the configuration depicted in Fig. 1 the Eq. (1) changes into the form:

$$\frac{\partial}{\partial z} \left( n \frac{\partial x}{\partial z} \right) = \frac{\partial n}{\partial x}, \quad (2)$$

$$\frac{\partial}{\partial z} \left( n \frac{\partial y}{\partial z} \right) = \frac{\partial n}{\partial y}, \quad (3)$$

integrating Eqs. (2) and (3) in both sides from  $\zeta_1$  to  $\zeta_2$ , it is obtained:

$$n \left( \frac{dx}{dz} \right)_{\zeta_2} - n \left( \frac{dx}{dz} \right)_{\zeta_1} = \int_{\zeta_1}^{\zeta_2} \frac{\partial n}{\partial x} dz \quad (4)$$

and

$$n \left( \frac{dy}{dz} \right)_{\zeta_2} - n \left( \frac{dy}{dz} \right)_{\zeta_1} = \int_{\zeta_1}^{\zeta_2} \frac{\partial n}{\partial y} dz, \quad (5)$$

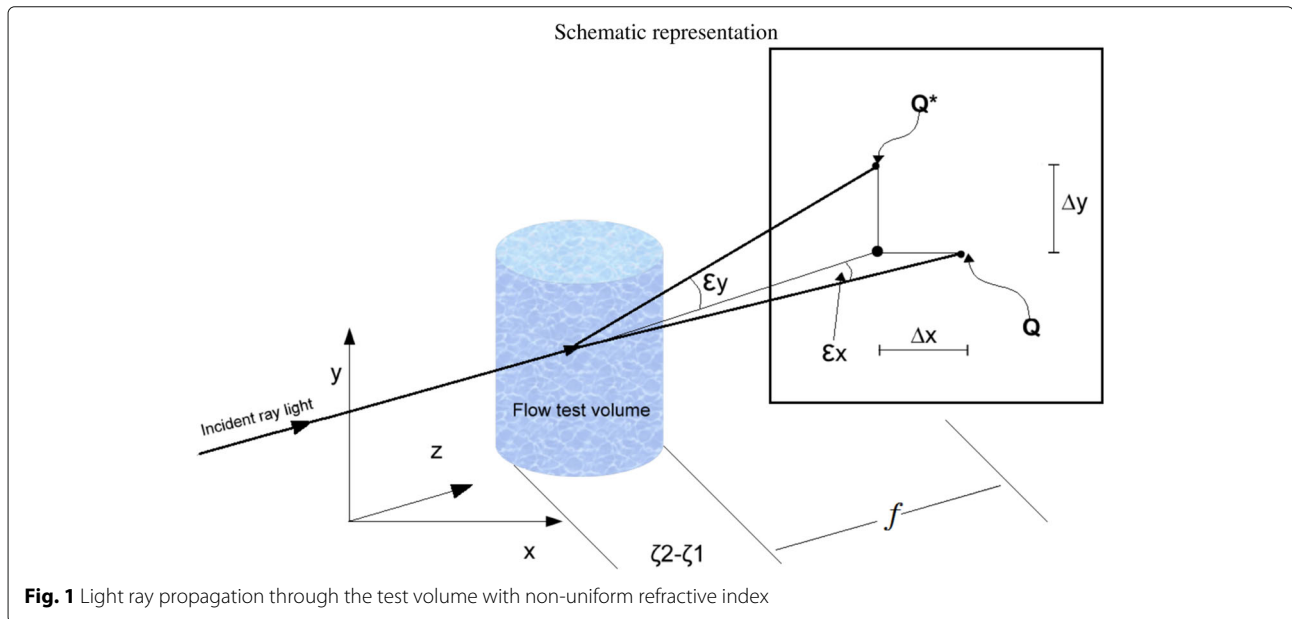
However, when the ray propagates through  $\zeta_1$  there is not deflection angle and then:

$$\left( \frac{dx}{dz} \right)_{\zeta_1} = 0 = \left( \frac{dy}{dz} \right)_{\zeta_1}, \quad (6)$$

as shown in Fig. 1. Substituting now the condition expressed in Eq. (6) into Eqs. (4) and (5) respectively, these change into:

$$\left( \frac{dx}{dz} \right)_{\zeta_2} = \frac{\Delta x}{f}, \quad (7)$$

$$\left( \frac{dy}{dz} \right)_{\zeta_2} = \frac{\Delta y}{f}. \quad (8)$$



where  $\Delta x$  and  $\Delta y$  are the infinitesimal displacements subtended by the angles  $\epsilon_x$  and  $\epsilon_y$  in the  $Z - X$  and  $Z - Y$  planes, respectively.

Considering hot gases from combustion in the flame as the object of study, it can be assumed that the information obtained in  $x$  direction is more significant than the corresponding information in the  $y$ -direction due to the cylindrical shape of flame. For this reason in this work, in Eq. (7) the  $x$  direction was used. Afterward, taking the approximation of small angle deviations  $\tan(\epsilon_x)$  can be changed by  $\epsilon_x$ . As shown in Fig. 1,  $\tan(\epsilon_x) = \Delta x/f$ , with  $f$  the focal length of the optical system which projects the image of the test volume, so using the approximation  $\epsilon_x = \Delta x/f$  as in [6] and employing Eqs. (4) and (7) it is obtained:

$$\epsilon_x = \int_{\zeta_1}^{\zeta_2} \frac{1}{n} \frac{\partial n}{\partial x} dz. \quad (9)$$

On the other hand, from the Gladstone-Dale relation  $(n - 1) = K\rho$ , it is possible to obtain  $\partial\rho/\partial x$  which can be substituted into Eq.(9) to get:

$$\frac{\partial\rho}{\partial x} = \frac{\delta x}{KWf}; \quad (10)$$

where  $K$  is the Gladstone-Dale constant which depends on the medium and the wavelength used in the measurement,  $\rho$  is the medium density,  $W$  is the object width,  $\delta x$  is the displacement in  $x$  direction when a light ray passes through an inhomogeneous medium, which is related linearly with the intensity obtained in the image plane according with Figs. 2 and 3,  $f$  represents the focal length of the second mirror. Integrating now the density field as described in the following equation:

$$\rho(x) = \rho_0 + \frac{1}{KWf} \int_{x_1}^{x_2} \delta x dx, \quad (11)$$

where  $\rho(x)$  is the density of hot combustion gases along the  $x$  axis and  $\rho_0$  is the nominal density of air at room temperature. This result is relevant because it can be used to get the temperature  $T(x)$  along the  $x$  axis using the following relation where  $T_0$  stands for the reference temperature:

$$T(x) = \frac{\rho_0}{\rho(x)} T_0. \quad (12)$$

As can be observed in Eq. (12) it is possible to obtain the temperature from a projection of the volumetric object, as was mentioned above. That is, in the two-dimensional projection of hot gases of flame there is intrinsic 3D information of the combustion process and its recovery is precisely the main objective of this work.

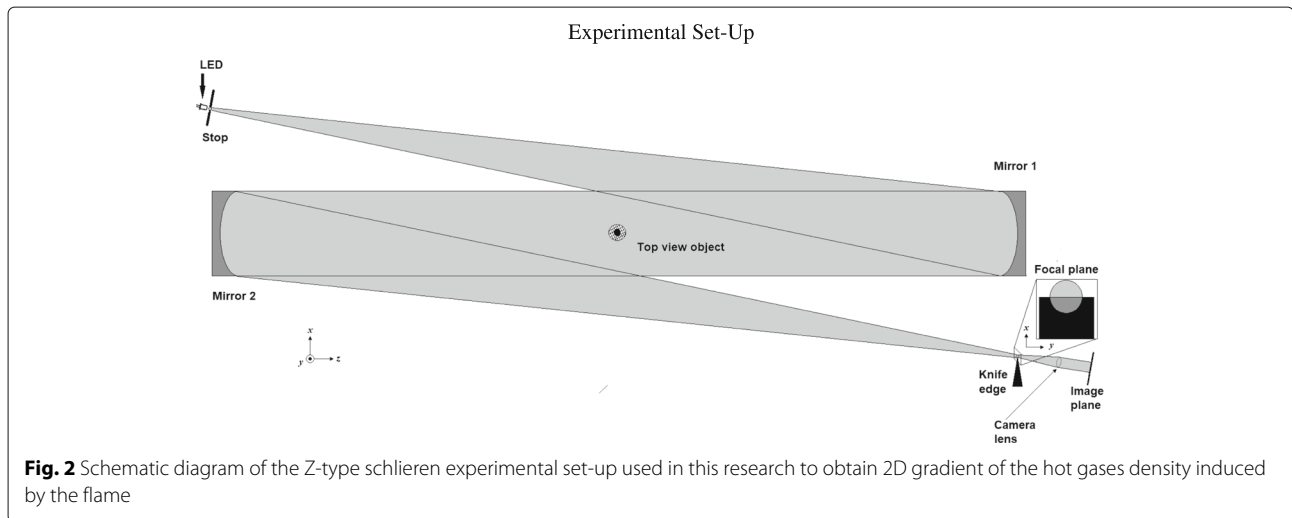
### 3D reconstruction of flame

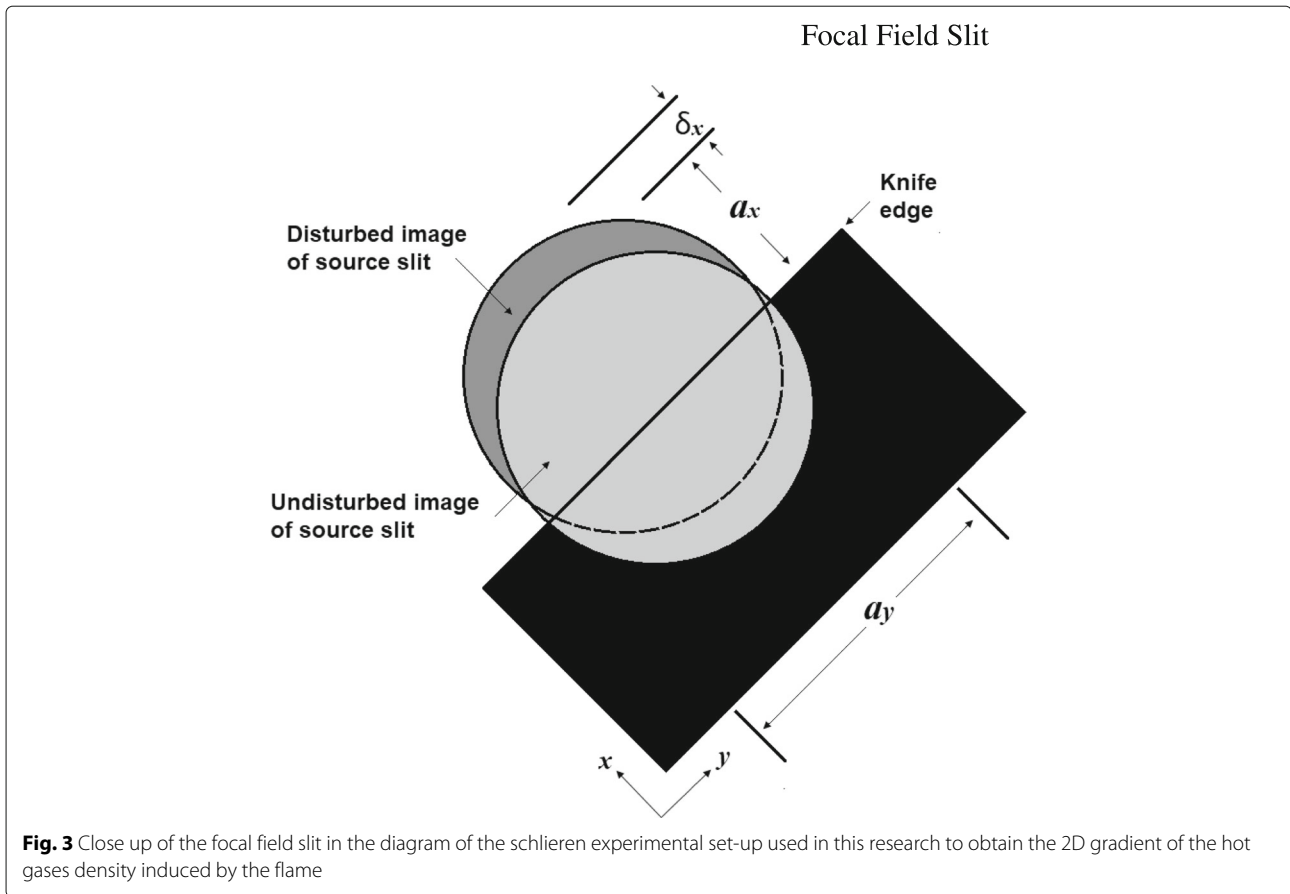
The temperature function depicted in Eq. (12) was obtained from the schlieren technique, depicted in Figs. 2 and 3, applied to the volumetric object with cylindrical symmetry using the Abel transform described by the relation:

$$g(x) = A \left[ \hat{f}(r) \right] = \int_x^\infty \frac{\hat{f}(r) r dr}{\sqrt{r^2 - x^2}}. \quad (13)$$

Where  $g(x)$  is the Abel transform of  $f(r)$ . Such that, to recover the 3D information, the inverse Abel transform should be used [7, 8]; several authors usually apply the inverse Abel transform to reconstruct a volume in three dimensions [7, 9–12]. The procedure proposed in this research for the 3D reconstruction is an alternative to the use of the Abel transform and additionally it is easy to implement, to achieve that purpose the outer product of two coordinate vectors  $x$  and  $y$  was applied using the next relation:

$$A = A + xy^t, A \in \mathbb{R}^{m \times n}, x \in \mathbb{R}^n, y \in \mathbb{R}^m, \quad (14)$$





being  $x$  and  $y$  skinny matrices, such that the number of columns of  $x$  is equal to the number of rows in  $y$ , as shown in the following example:

$$xy^t = (1, 2, 1) \begin{pmatrix} 1 \\ 2 \\ 1 \end{pmatrix}. \quad (15)$$

In this work, the  $x$  coordinate represents a row of temperature field associated to a height of flame, and  $y^t$  represents the transpose of  $x$  coordinate matrix [10]. Then using Eq. (15) the temperature slices at a specific height were obtained. Finally, doing a concatenation of all the temperatures slices, the flame volume was reconstructed.

So, under the cylindrical symmetry hypothesis, the shape of flame  $h$  at a specific  $x$  coordinate was obtained making a Gaussian fitting to the curve given by:

$$h(x) = ae^{-(x-b)^2/2c^2}, \quad (16)$$

where  $a$ ,  $b$  and  $c$  were calculated for each  $x$  coordinate, by means of minimizing the mean squared error between the estimated curve and the experimental data as shown in Fig. 8a, b, c and d.

On the other hand, it is well known that a fitting process introduces an absolute error [8], for this reason in order

to validate the approximation used, the mean square error between the fitted curve and the experimental data was computed. The functions  $h(x)$  and Abel transform  $g(x)$  theoretically give the same shape when they are applied in one dimension, that means, both give the projection of light sheet that passes through a cylindrical transparent media cutting a circular slice. These functions describe the temperature profile in  $x$  direction obtained with the schlieren technique.

## Results

### 2D flame reconstruction process

Figure 2 shows the top view of Z-type schlieren experimental set-up which includes a white light diode as light source, a stop metallic sheet with a hole of two mm diameter to define the dynamic range of the schlieren setup, two spherical mirrors with a diameter  $D = 0.15m$  and a focal distance  $f = 1.54m$ , and a knife edge located at the focal plane. According to the experimental set-up, the knife edge is placed at the focal plane in vertical position to be displaced along the  $x$  direction perpendicularly to the  $z$  axis as shown in Fig. 3 where is described a small displacement  $\delta x$  which produces an intensity change at the image plane located at the camera position. The

procedure to evaluate  $\delta x$  is important because it is related with the intensity in the image plane and with the sensitivity of the schlieren set-up. In this research, the knife edge is displaced along the  $x$  direction with small increments  $\delta x$  to achieve an image with a half of the diameter intensity at the focal plane. Once the knife edge was located at the required position it was fixed, so that a half of intensity was stopped, and a half of intensity crossed the focal plane to arrive at the image plane. At this fixed position of the knife edge, the schlieren images were captured. The brightness in schlieren images was evaluated qualitatively, by this reason, normalized temperature fields were also obtained. In this research, an optical calibration of the schlieren system was not done. In turn, the changes in the light intensity detected by the camera allow to obtain the gradient of hot gases density as shown in Fig. 5. To form the intensity images a luminera digital camera was used with a navitar lens with a focal length of  $= 50\text{mm}$ . The camera provides 30 frames per second with  $640 \times 640$  pixels. The burner was located in the middle of the schlieren set-up and the hot gases produced by the combustion flame flow in vertical direction, the same direction in which is positioned the knife edge so the schlieren set-up can be sensible in the  $x$  direction [13].

Four experimental conditions labeled as “One Open Slot”, “Two Open Slots”, “Three Open Slots” and “Four Open Slots”, which will be called 1OS, 2OS, 3OS and 4OS respectively, were considered. The experimental condition “One Open Slot” describes the fact that only one slot (hole) was opened in the burner that produce the flame, “Two Open Slots” describes the case where two slots were opened in the burner and so on. In the acquisition procedure of the data sets, the pressure of gas admission to the burner was controlled and adjusted frequently to assure the most similar experimental condition in the gas burning in every case considered. Figure 4 shows a photograph of the gas butane burner used in this research, at the bottom are shown the circular holes (slots) that allow the admission of the air to the burner. Each experimental condition considered by the schlieren technique produced a data set associated with a mesh containing the intensity distribution of temperature associated with each pixel in the flame image. The processing of the data acquired finally allows the 3D reconstruction of flame.

Figure 5, shows the gradient of the hot gases density obtained from the schlieren measurements corresponding to the experimental conditions 1OS, 2OS, 3OS, and 4OS of air admission in the burner, respectively. As can be observed in Fig. 5, the gradient distribution of hot gases has some own characteristics associated to each experimental condition considered, for example, the 2D flame shape tends to be more symmetric keeping a cylindrical geometry for the cases corresponding to an

even number of opened slots. It is also noticeable how the reaction zone shape depends on the premixed air-fuel quantity as is described by the conical structures located at the base and close to the center of flame. Figure 6 shows processed images of the original 2D data projections shown in Fig. 5 obtained from the schlieren technique for the experimental conditions: a) One Open Slot (1OS), b) Two Open Slots (2OS), c) Three Open Slots (3OS), and Four Open Slots (4OS). In Fig. 6 the temperature intensity distribution was normalized using the schlieren temperature intensities,  $T$ , employing the relation:  $T_{normalized} = (T - T_{min}) / (T_{max} - T_{min})$ , where  $T_{min}$  is the minimum intensity of temperature and  $T_{max}$  is the maximum intensity of temperature. Then, the normalized temperature distribution was highlighted employing a colors gamma which goes from blue (cold) to red (hot). This normalization procedure described before was also used to represent Figs. 7 and 8.

### 3D flame reconstruction process

Once the reconstruction of the flame in two dimensions was performed, the reconstruction of the flame in three dimensions was carried out, for which it was necessary to applying the outer product of each coordinate row by itself. In the first step of the flame reconstruction process in 3D, it was obtained a 2D Gaussian shape for each height and then were concatenated each one of these slices to obtain the complete volume. This reconstructed volume represents the temperature distribution in 3D as shown in Fig. 7 for the four sets 1OS, 2OS, 3OS and 4OS, being the temperature intensity in the flame described by colors going from blue (cold) to red (hot). In Fig. 7 the new  $x$  and  $z$  axis correspond to the original  $x$  and  $y$  axis of the experimental data, respectively. The new axis obtained due 3D reconstruction was called rotation axis (new  $y$  axis) in order to avoid confusion. It is important to note that the flame reconstruction process expands the information on the particular characteristics of the flame with respect to the two-dimensional image originally measured.

### Error estimation in the 3D reconstruction process

In order to estimate the error in the three-dimensional reconstruction process of the flame studied in this research, regarding the assumption of cylindrical symmetry of temperatures in the flame along the vertical axis or axis of rotation, a numerical fitting was made, (assuming a Gaussian distribution of the temperature in the flame at various heights fixed), to the data entered to reconstruct the volume obtained directly from the experimental measurements made using the schlieren technique. Several slices were considered at fixed heights in the flame corresponding to the pixels marked in Fig. 8a, b, c and d, which are shown in Fig. 8e, f, g and h, respectively. The absolute mean error by discrepancy between the fitted Gaussian



### Burner Thermocouple.



**Fig. 4** Photograph of the gas butane burner used to perform the measurement of temperatures of flame. In the photograph are shown at the bottom the circular holes (slots) that allow the admission of air to the burner and at the top the tip of the thermocouple used to measure the temperature in the flame

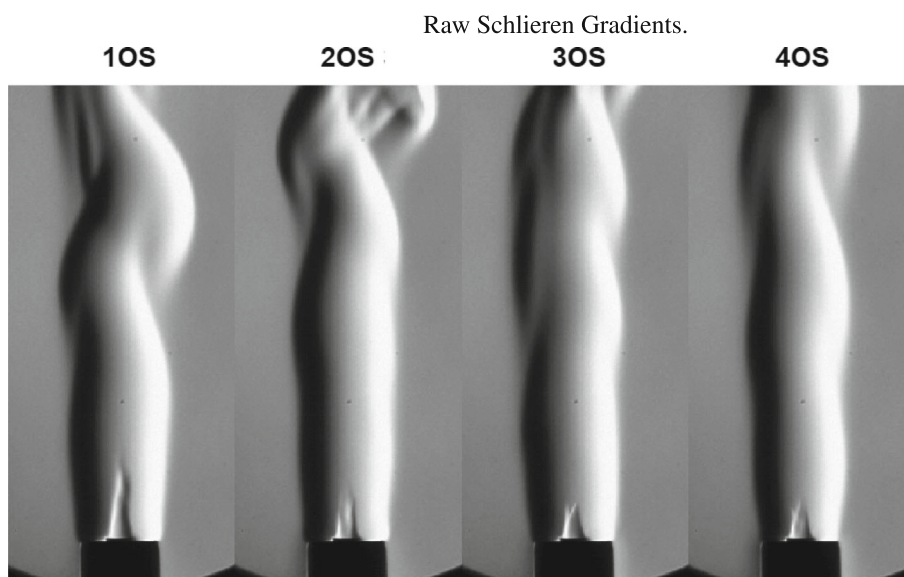


**Fig. 5** Gradient of the density of hot gases obtained from the schlieren measurements corresponding to the experimental conditions 1OS, 2OS, 3OS and 4OS air intake at the burner, respectively. The gas reaction zone depends on the amount of premixed air fuel as is described by the conical structures located in the base and close to the center of the flame

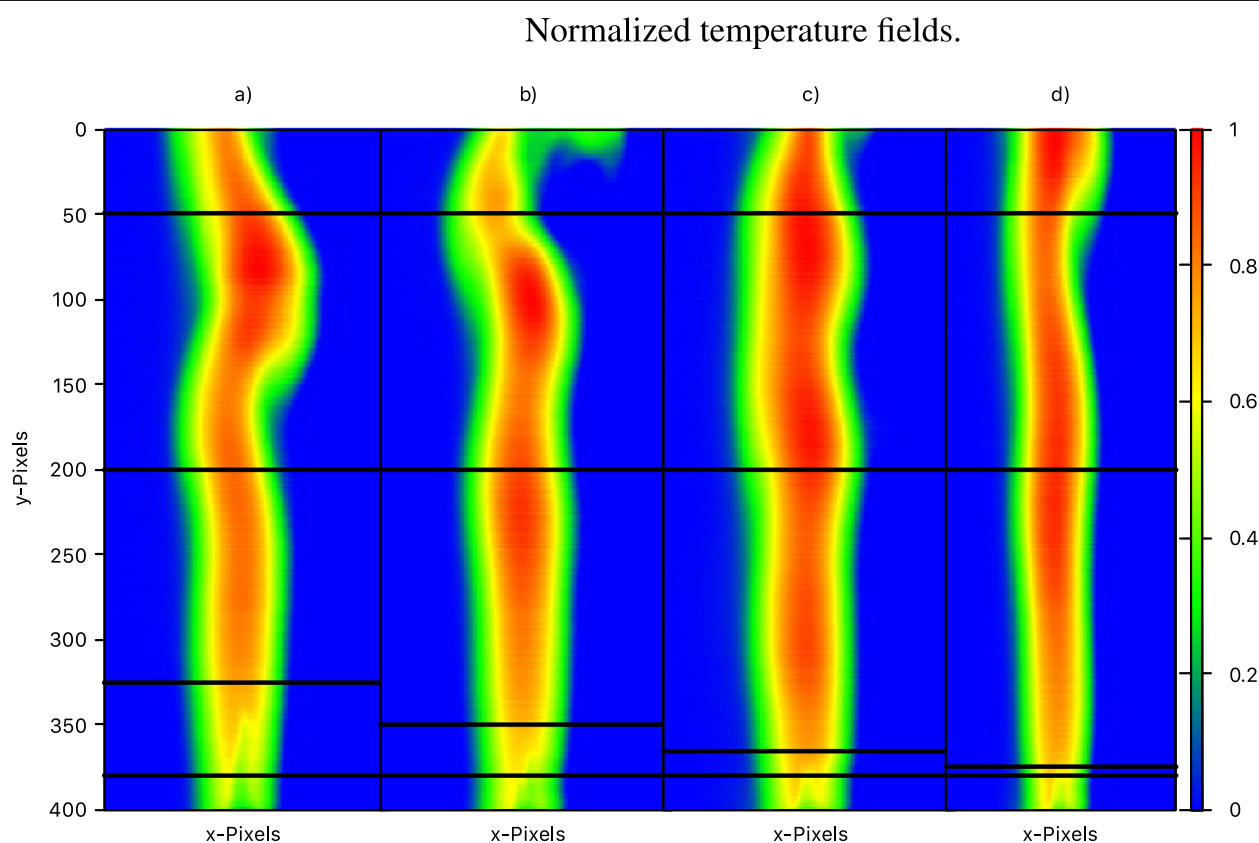


**Fig. 6** Processed images of the original 2D data projections shown in Fig. 5 obtained from the schlieren technique for the experimental conditions: **a)** One Open Slot (1OS), **b)** Two Open Slots (2OS), **c)** Three Open Slots (3OS), and **d)** Four Open Slots (4OS). Colors correspond to the temperature intensity distribution which goes from blue (cold) to red (hot). The horizontal black lines in the images represent different height of the flame at which were obtained slices of the temperature distribution on a horizontal plane as shown in Fig. 8

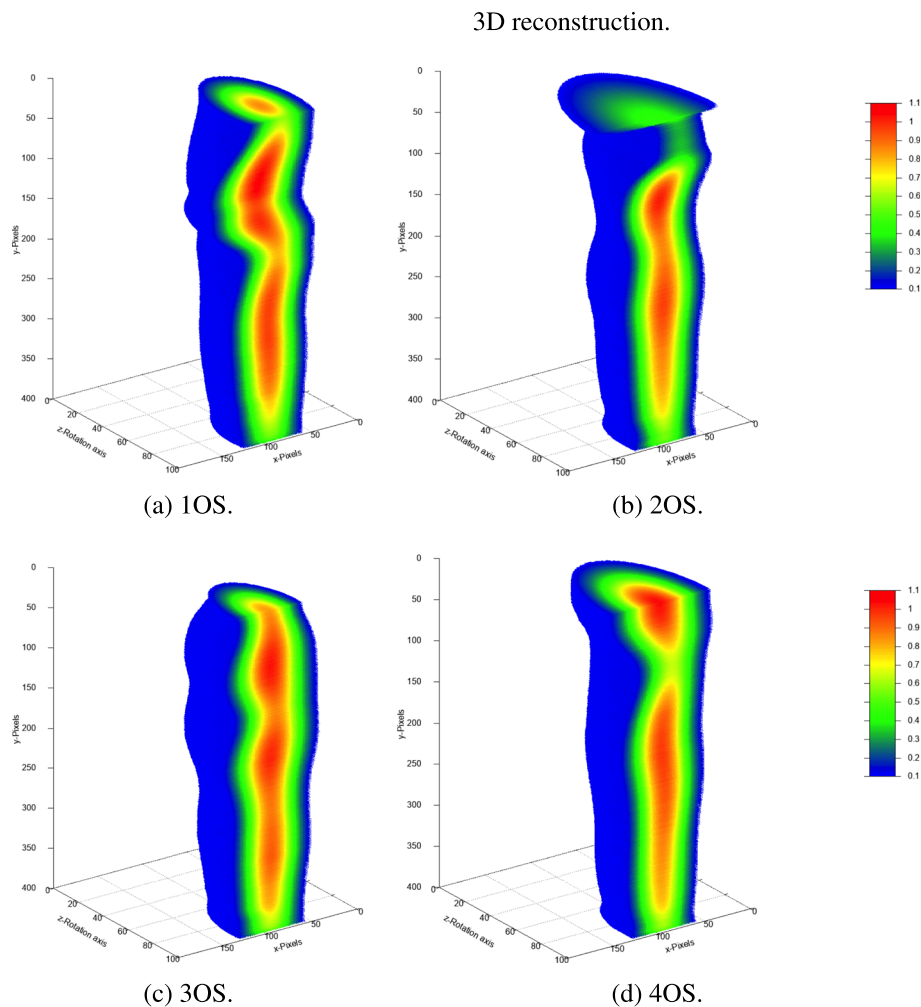


**Fig. 7** Slices of the reconstructed 3D volume of a flame (the cuts were made at the half value corresponding to pixel 100 at the x axis). The reconstructed volume of flame represents the temperature distribution in 3D for the four data sets: **a)** 1OS, **b)** 2OS, **c)** 3OS and **d)** 4OS, colors correspond to the temperature intensity which goes from blue (cold) to red (hot). The x and z axes correspond to the original x and y axes of the experimental data, respectively. The new axis obtained due to the 3D reconstruction is the rotation axis

curve for each the 400 rows selected on a fixed value on the  $y$  axis and the experimental data computed for each one of the 400 slices constituting the flame are quite small as shown in Fig. 9 for some representative cases. Nevertheless, in Fig. 8b) corresponding to the 2OS condition, the mean error rise at the beginning of the graph as a consequence of the perturbations occurring at the top of the experimental data reconstruction as shown in Figs. 5b) and 6b). Although, it is important to note that the data set associated to the perturbations appearing at the top of flame shown in Fig. 5b) are far away from the hottest area which makes possible to ignore it. Disregarding the disturbance described at the beginning of Fig. 9b, in general terms the mean error was less than 0.04, which means that the reconstruction process was made with an accuracy estimated around 96%. Thus, all calculations performed in

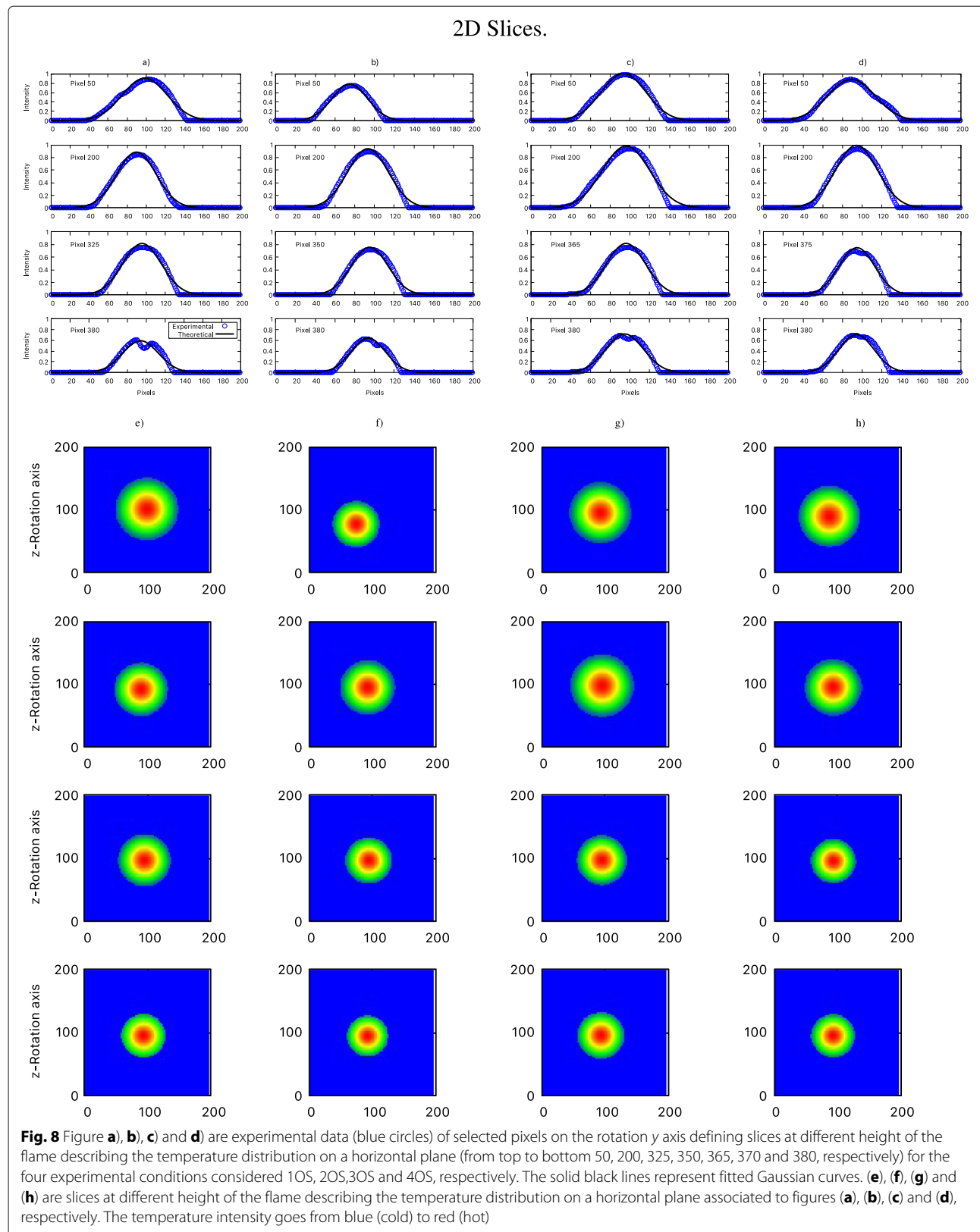
this research confirm the validity of our hypothesis about the cylindrical behavior of the temperature distribution in the flame.

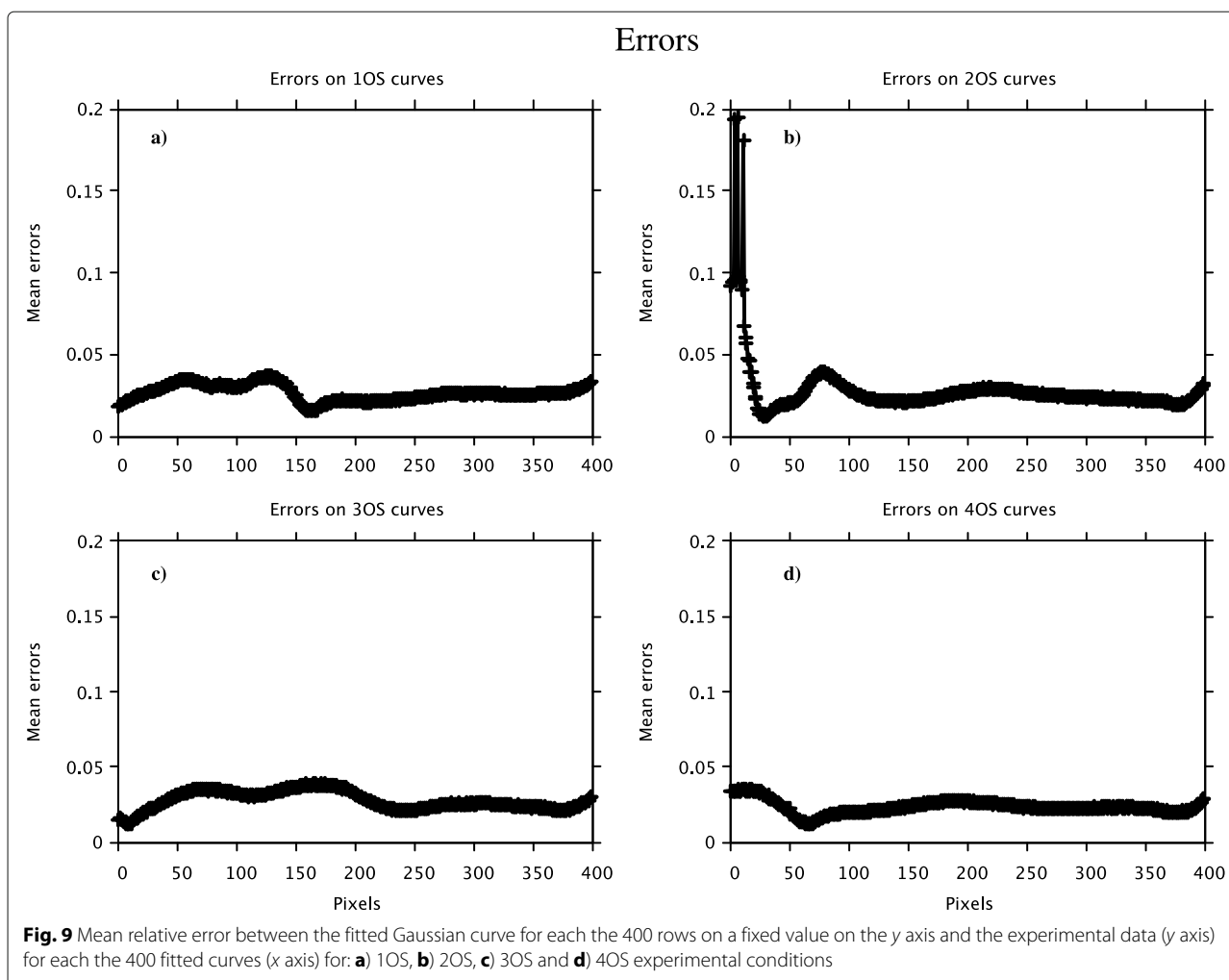
### Temperature distribution measurement

#### *Temperature measurement in the flame using a thermocouple*

In this research was also performed the measurement of temperature distribution of flame in order to validate again the assumption of cylindrical symmetry. The temperature measurement was completed for the four conditions (1OS, 2OS, 3OS and 4OS) considered in this work, using a K type thermocouple as measurement probe connected to a 2110 KEITHLEY digital multimeter. The temperature was measured at three specific heights of flame respect to the base of the butane gas burner for







each experimental condition considered. The thermocouple was attached to a vertical translation base supported on a rail that allowed a horizontal translation to perform a sequential sweep of observation points every two millimeters along a sampling line at a specific height of flame. Figure 10 shows the temperature distribution as a function of the spatial coordinate  $x$  in the horizontal direction, measured at three different heights of flame respect to the bottom of the flame in the gas burner position for 1OS, 2OS, 3OS and 4OS experimental conditions. The zero position ( $x = 0$ ) represents the center of the burner. As can be seen in Fig. 10a the flame for 1OS condition has a temperature distribution with a slight asymmetry and presents a shift toward the right of the center of the burner due to the air admission for the combustion comes from a side entry of the burner corresponding to the “One Open Slot” condition. In the case of 2OS condition shown in Fig. 10b, the temperature distribution in the flame presents a better symmetry around the center of the burner respect to the behavior found for the 1OS condition. As can be seen in Fig. 10b the

temperature distribution measured at the lowest height (0.5 cm) respect to the burner position and located under the flame reaction zone shows a valley reaching a minimum around the  $x = 0$  position. This behavior is due to the fresh mixture of air and butane gas admitted to the burner has not yet reacted. Figure 10c corresponding to the 3OS condition shows a high symmetry in the temperature spatial distribution around the burner position describing approximately a Gaussian distribution shape. Clearly the air admission using three open slots (3OS) brings on high stability to the combustion process. It is interesting to comment that the temperature reached by the flame ( $\approx 390^\circ\text{C}$ ) for the minimum height considered (0.5 cm) at  $x = 0$  in the 3OS condition was higher than the value measured at the same height for the 2OS experimental condition. Finally, in the case of 4OS experimental condition it is possible to say that the temperature spatial distribution of flame maintains a good grade of symmetry around  $x = 0$ . Furthermore, in the 4OS experimental condition was verified a remarkably interesting behavior of the temperature distribution for the minimum height

## Thermocouple Temperature Measurement.

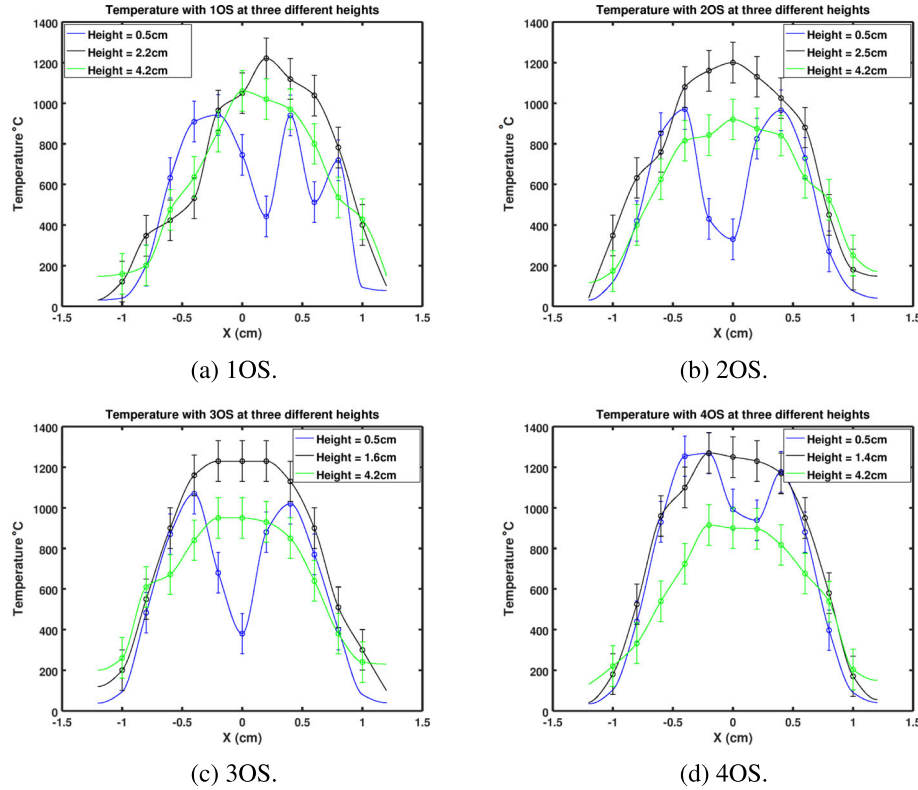


**Fig. 10** Temperature distribution as function of the spatial coordinate  $x$  in the horizontal direction, measured at three different heights of flame respect to the bottom of the flame in the gas burner position for the experimental conditions: **a)** 1OS, **b)** 2OS, **c)** 3OS and **d)** 4OS. The zero position ( $x = 0$ ) represents the center of the burner. The solid lines were obtained by interpolation and are only for eye-guide

considered (0.5 cm) at  $x = 0$ ; the flame reached temperature values at  $x = 0$  (corresponding to the valleys) higher than those reached at the maximum height considered (4.2 cm) which was a behavior not found in any other of experimental conditions considered. The temperature spatial distribution corresponding to the 4OS condition still shows a valley shape around  $x = 0$  for the measurements done at the minimum height considered (0.5 cm) such as in the other experimental conditions considered but at higher temperatures than those obtained in the conditions 1OS, 2OS and 3OS. In fact, it is interesting to note that the highest temperatures in the flame were reached in some positions of the  $x$  coordinate the highest temperatures reached by the flame.

#### Temperature measurement from schlieren technique

The temperature distribution of flame was also obtained from schlieren technique for one of the representative cases considered in this work. Figure 5 shows the gradient of the hot combustion gases density obtained from the schlieren measurements corresponding to the experimental conditions 1OS, 2OS, 3OS and 4OS of air admission

in the burner generating the flame. As can be observed in Fig. 5 it is easy to appreciate the hot gases distribution in the flame in each experimental condition, via the variations of the hot gases density. In fact, it is interesting to observe the gases reaction zone described by the conical structures located at the base and close to the center of flame in Fig. 5. The size of these conical structures depends on the premixed air-fuel quantity.

The temperature distribution of flame was obtained calculating first the density of hot gases along the  $x$  direction using the Eq. (11) listed in section 2.1 and then substituting it into Eq. (12). Figure 11 shows a comparison of the temperature spatial distribution at a height of 1.4 cm, respect to the base of the burner corresponding to the 4OS experimental condition, obtained by the schlieren technique and the measurements done with the K type thermocouple. Then, for the same height position in schlieren normalized temperature,  $T_{normalized}$  was calibrated with the temperature measured with a thermocouple, using the thermocouple maximum temperature,  $T_{Thermocouple,max}$  and the thermocouple minimum temperature corresponding to room

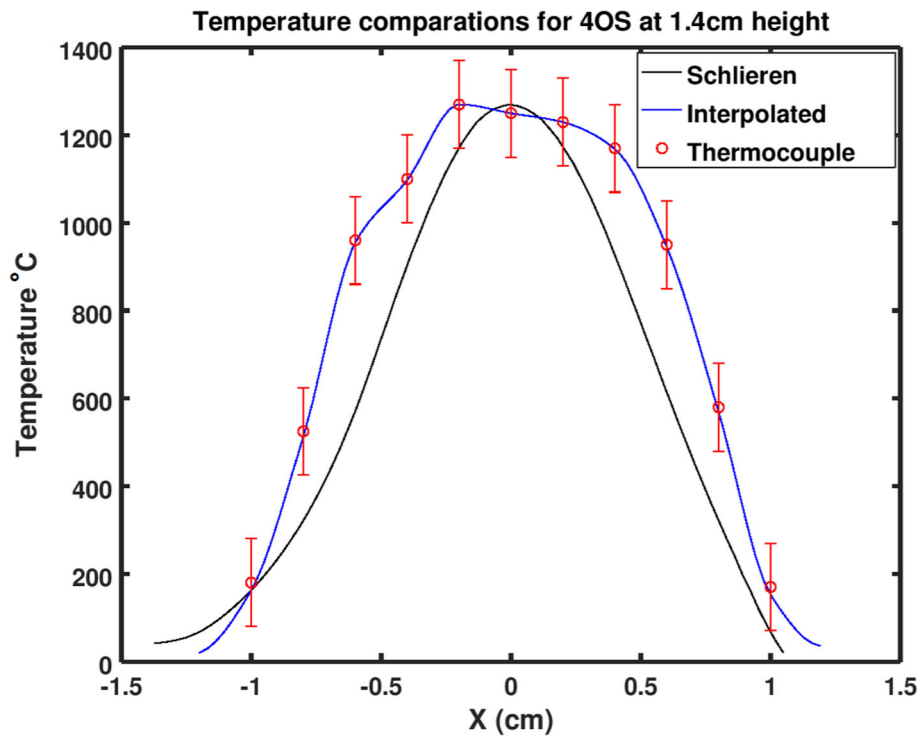


**Fig. 11** Comparison of the temperature spatial distribution at a height of 1.4 cm, respect to the base of the burner, for the 4OS experimental condition, obtained by the schlieren technique and the measurements done with the K type thermocouple. Both temperatures measurements are very similar considering the uncertainty bars associated to the values obtained using the thermocouple. The continuous line joining points measured with a thermocouple was obtained by interpolation and is only for eye-guide

temperature  $T_{Thermocouple,min} = T_0 = 20^{\circ}C$ , using the relation  $T_{calibrated,schlieren} = T_{normalized}(T_{Thermocouple,max} - T_0) + T_0$ . The calibration in  $x$  direction was done with a Pixel size of  $Pix = 0.031053cm$  to scale the  $x$  axis in centimeters. To help to visualize the behavior of the temperature points in the flame measured with the thermocouple, an interpolation procedure using the Octave function `interp1` with Piecewise Cubic Hermite Interpolating Polynomial (*pchip*) was performed.

As shown in Fig. 11 there is a good agreement between the flame temperature data obtained from the schlieren measurements and the direct measurements using a thermocouple. The agreement between both temperatures measurements is good if it is taken into account the uncertainty shown in Fig. 11 associated with the values obtained using the thermocouple.

## Conclusions

In this research was developed a three-dimensional reconstruction of a flame from two-dimensional temperature measurements obtained from the gradient of hot gases density using an easy and efficient method based on the schlieren technique. The reconstruction process was based on the hypothesis of cylindrical symmetry of the

temperature spatial distribution in the flame. The method proposed in this work to reconstruct the 3D characteristics of flame, only requires the calculation of the outer product between one sample row of the temperature field and its own transpose sample row of the temperature field to obtain one slice of the temperature of the flame. Once it has been obtained a collection of temperatures slices, it can be reconstructed the temperature distribution in the volume of flame. The mean error was evaluated in the calculations of temperature intensity for each flame under the cylindrical symmetry assumption and was obtained an accuracy of 96% when they were compared to a Gaussian distribution. The temperature distribution of flame obtained from schlieren measurement was calculated and it was found a good agreement between these calculations and direct measurements of the flame temperature using a thermocouple.

## Acknowledgements

First and second author would like to thank CONACYT, Facultad de Ingeniería, UACH and PRODEP for the support given to this project.

## Authors' contributions

CAH design of the work, AND the acquisition, analysis, AND interpretation of data AND have drafted the work or substantially revised it. JLHA the acquisition, analysis, AND interpretation of data AND have drafted the work or

substantively revised it. DMH design of the work, AND the acquisition, analysis, AND interpretation of data. AVCG interpretation of data AND have drafted the work or substantively revised it. JGMR interpretation of data AND have drafted the work or substantively revised it. The author(s) read and approved the final manuscript.

#### Funding

Not applicable.

#### Availability of data and materials

The datasets used and/or analyzed during the current study are available from the corresponding author on reasonable request.

#### Competing interests

The authors declare that they have no competing interests

#### Author details

<sup>1</sup>Facultad de Ingeniería, Universidad Autónoma de Chihuahua, Nuevo Campus Universitario, Circuito Universitario S/N, 31125, Chihuahua, Chih., México. <sup>2</sup>Centro de Investigaciones en Óptica A.C., Lomas del Bosque 115, Lomas del Campestre, León, C.P. 37150, Guanajuato, México. <sup>3</sup>Centro de Investigación en Materiales Avanzados S.C., Miguel de Cervantes 120, C.P. 31136, Chihuahua, Chih., México.

Received: 5 November 2019 Accepted: 5 August 2020

Published online: 03 September 2020

#### References

1. Vanek, FM, Albright, LD: Energy Systems Engineering Evaluation and Implementation. McGraw-Hill, United States of America (2008)
2. Merzkirch, W: Flow visualization. 2nd edn. Academic Press, Inc, Orlando (1987)
3. Settles GS: Schlieren and Shadowgraph Techniques. 1st edn. Springer, Berlin (2001)
4. Deans, SR: The radon transform and some of its applications. John Wiley & Sons, Ltd, New York (N.Y.) (1983)
5. Weisstein, EW: Second edition CRC concise encyclopedia of mathematics. CHAPMAN & HALL/CRC, Boca Raton (2003)
6. Hanson, KM, Wecksung, GW: Local basis-function approach to computed tomography. *Appl. Opt.* **24**, 4028–4039 (1985)
7. Dribinski, V, Ossadtchi, A, Mandelstam, VA, Reisler, H: Reconstruction of Abel-transformable images: The Gaussian basis-set expansion Abel transform method. *Rev. Sci. Instrum.* **73**(7), 2634–2642 (2002)
8. Jain, AK: Fundamentals of digital image processing. Prentice-Hall, Inc, Upper Saddle River, NJ, USA (1989)
9. De La, Rosa-Miranda, E, et al: An alternative approach to the tomographic reconstruction of smooth refractive index distributions. *J. Eur. Opt. Soc. Rapid Publ. Eur.* **8**, 13036 (2013). ISSN 1990-2573
10. Golub, GH, Van Loan, CF: Matrix computations. 3rd Ed. Johns Hopkins University Press, Baltimore, MD, USA (1996)
11. Press, WH, Teukolsky, SA, Vetterling, WT, Flannery, BP: Numerical Recipes 3rd Edition: The Art of Scientific Computing. 3ed. Cambridge University Press, New York, NY, USA (2007)
12. Sen, A, Srivastava, M: Regression analysis: theory, methods, and applications. Springer Science & Business Media (2012)
13. Alvarez-Herrera, C, Moreno-Hernández, D, Barrientos-García, B: Temperature measurement of an axisymmetric flame by using a schlieren system. *J. Opt. A Pur. Appl. Opt.* **10**, 10 (2008). <https://doi.org/10.1088/1464-4258/10/10/104014>

#### Publisher's Note

Springer Nature remains neutral with regard to jurisdictional claims in published maps and institutional affiliations.

**Submit your manuscript to a SpringerOpen<sup>®</sup> journal and benefit from:**

- Convenient online submission
- Rigorous peer review
- Open access: articles freely available online
- High visibility within the field
- Retaining the copyright to your article

---

Submit your next manuscript at ► [springeropen.com](https://www.springeropen.com)